

Effect of Closely Spaced Knots on the Failure Mechanism of Timber Beams

Khaled Saad, András Lengyel*

This research presents a parametric three-dimensional finite element study on the effects of closely spaced knots and related fibre deviations on the flexural failure mechanism of wood beams. The model considers the effects of the position of the knots along the beam's longitudinal and vertical axis. The numerical models were validated by bending tests performed on six timber beams. The actual three-dimensional geometry of knots and related fibre deviations were determined accurately based on an algorithm proposed previously by the authors. The elastic-plastic constitutive law of Nordic Spruce wood was considered based on the Hill anisotropic model. The failures were numerically predicted with the help of the Tsai-Wu failure criterion. The validated numerical models can also be used based on visual inspections. The user needs only to define the position and size of the knots and the space between them. Moreover, the model allows defining different fibre patterns in the knot vicinity. The model considers a fixed knot located in the tension zone at the mid-span of the beam and a moving knot adjusted at horizontal and vertical centre-to-centre distances d and v from the fixed one. Results revealed that regardless of the distance d (where $v = 0$), the failure will initiate at the same load levels for both knots. However, moving the adjacent knot diagonally (v not equal to 0) causes shear failure between the knots. The part of the clear wood between the knots is ineffective if the knots' centre-to-centre distance is less than three times the knot diameter.

Introduction

The finite element approach is used primarily in timber numerical modelling. On the one hand, computational models must be fine-tuned to anticipate the three-dimensional state of stresses due to wood's anisotropic and complex behaviour. In compression, wood follows the elastic-plastic constitutive law, yet in tension parallel to the grains, it is brittle [1-3]. Elasticity describes an element's capacity to deform under moderate stress and then return to its original undeformed shape once the load is removed. Furthermore, compression plastic deformation or tensile failure will occur when subjected to a higher loading value. Tension is a common cause of timber component failure; it causes the beam compression zone's plastic capacity to be underutilized [4]. The ultimate flexural capacity of timber structural components has been predicted in several approaches [5-7]. The Tsai-Wu strength hypothesis is the most accepted failure criteria for estimating the ultimate load-bearing capacity of anisotropic materials.

Tests are frequently used to derive material constants for numerical analysis. The wood properties vary widely based on various factors, including species, age, moisture content, density, and location. Properties can also vary from one sample to another and are frequently mainly indicative [8-11]. The elastic limit in tension and the material's nonlinear compression behaviour are key characteristics of the overall bending behaviour.

In terms of stress-strain characteristics, failure modes, and preferred fibre orientation, wood anisotropy is analogous to transversely isotropic fibre-matrix composite material anisotropy, although it is more sophisticated. Fortunately, the linear orthotropic material model with nine material constants may be utilized to characterize the elastic behaviour of wood at any time. Several earlier researchers have examined the difficult behaviour of wood beams by developing linear and nonlinear mechanical models based on experimental data and using the finite element method (FEM), which is a reliable numerical method [12-16]. The application of constitutive models with appropriate material characteristics is required for numerical analysis. Timber requires a more sophisticated definition than fibre-reinforced composites, which are frequently linearly orthotropic elastic with brittle rupture. Unfortunately, the linear orthotropic model is only applicable in the linear

Structural Mechanics Department, Faculty of Civil Engineering,
Budapest University of Technology and Economics, Műegyetem rkp.
3, Budapest, 1111, Hungary

*Corresponding author:
E-mail: khaled.saad@emk.bme.hu; Tel.: +36704171095

DOI: 10.5185/amlett.2022.031702

range. Beyond that, nonlinear stress-strain relationships are required, especially in the compression area, where a variety of different types, such as totally plastic, have been used (e.g. [17,18]), bilinear (e.g. [19-21]), higher-order (e.g. [22]). A tri-linear stress-strain diagram was proposed to evaluate the failure behaviour of wood under compression parallel to the grain [23]. Hill also suggested a bilinear anisotropic stress-strain relationship that may be used to estimate orthotropic linear elastic-quasi-rigid in tension and orthotropic linear elastic-perfectly plastic or bilinear in compression where two straight lines represent the stress-strain curve's plastic component with differing slopes [24-27]. See Fig. 1 for model illustrations. More suggested models can also be found in [28,29].

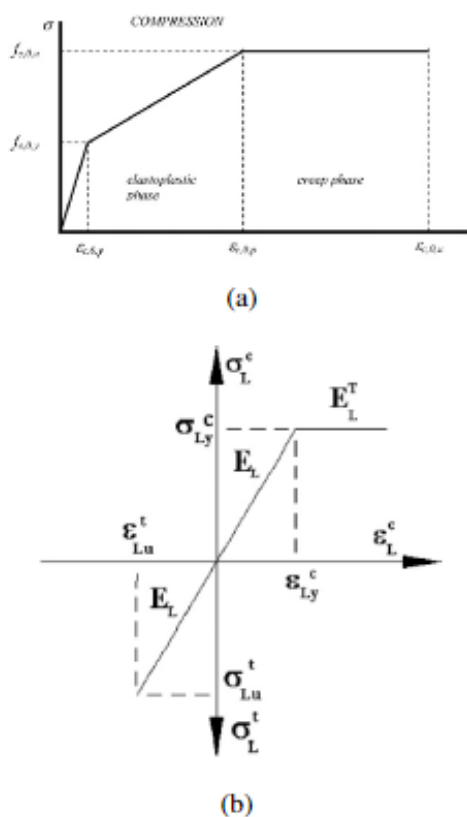


Fig. 1. Stress-strain relationship for wood under tension and compression parallel to the grain. (a) compression parallel to grain as suggested by [25], (b) [30].

As a function of the Euler's angles (λ, ρ), an investigation was carried out to analyze the changes in the elastic properties of wood members in the L.T. and L.R. planes, represented as a material that is linearly elastic and orthotropic, as well as several tests [31,32]. The finite element approach was used to analyze the behaviour of spruce (*Picea abies*) wood beams, and the Generalized anisotropic Hill model was proposed. Three-point static bending and compression tests were used to validate the model and determine the characteristics of the material being studied [33].

Knots and related grain deviations are the most prevalent natural flaws, and they reduce the overall capacity of wood components [34]. Knots reduce tensile strength owing to grain deviation and stress redistribution, although compression strength parallel to the undisturbed grain direction is unaffected. There are two sorts of knots: "dead knots" are no longer attached to the main body of wood, and "live knots" are still attached to the main body of the wood. Furthermore, undergrown knots are more prone than dead knots to cause grain deviation and tension loss. The material properties of wood, such as strength and stiffness, are greatly influenced by global and local fibre deviations. They also cause a localized stress concentration, resulting in early tensile failure and poor compression capability usage [35]. The longitudinal tensile strength, MOR, compression strength parallel to the grain, and MOE are the most concerning parameters. Knots usually cause stress discontinuities in their surroundings and a tangential plane deviation of the surrounding fibres (L.T.). The knot's inhomogeneity with the surrounding wood composition will also contribute to the loss of strength. Furthermore, the knotted wood's density is double that of the knot-free wood's average density.

Several non-destructive methods, such as the laser confocal microscope, can be used to assess fibre deviations [36], the application of the tracheid effect scanning [37], X-ray scanning technique [38], the CT-direction process (Computed Tomography) [39]. Mathematical models were also designed to describe the principles of branch and knot generation [40-42]. To construct a 2D in-plane pattern for the knots, grain angles, and density variations, an x-ray scanner was used. The out-of-plane component (diving angles) was not, however, assessed. Knots spaced at least 200 mm apart were proven to decrease stiffness more effectively than a single knot. Forty-four specimens of lumber were evaluated under tension to determine tensile strength; the pith was detected in 44% of the observed failed parts, whereas knots in the centre of the wood section were identified in 10% of the failure sections [38]. [37] proposed a non-destructive approach to creating the 3D fibre pattern for the Norway spruce timber by investigating the relationship between the diving angle and the grayscale image of the reflected light by applying the tracheid effect scanning to identify the in-plane and out-of-plane angle (fibre direction) in the knot vicinity. The models were verified by the mathematical model created by [42]. The behaviour of Scots pine (*Pinus Sylvestris*) wood was investigated using transversally isotropic 3D finite element models (five independent material characteristics for the elastic behaviour). The authors provided a 3D analytical wood material model to predict the behaviour of defected timber beams while taking into account the impacts of any existent elliptical, rotating, and oblique cones as a representation of the knots. The knots generate a discontinuity in the stress distribution, which causes the strength to be reduced. Shear and perpendicular to grain stress components emerge in the fibres around the knots.

Parallel to fibre stresses, these stresses are more significant. Furthermore, different Young's moduli (E_c and E_t) were explored for tension and compression.

A 3D flow-grain analogy was used in another study to compute the grain deviation in the knot vicinity, which involved making the knot's contour a solid barrier while running laminar flow through the beam and measuring the velocity components in each element [43]. The 3D flow-grain analogy is an approach in which laminar flow flows through the specimen, turning the knots into solid barriers; instead of generating a mesh in the shape of the streamlines, the elementary Cartesian velocity components are recorded. After that, a solid analysis will be carried out. Solid elements will be used to replace fluid components, and the fibre deviation will be computed using velocity vector relationships. The wood is surrounded by a fluid-filled top prismatic pipe, with knots functioning as the fluid's wall boundaries.

The impacts of fibre orientations and knots on the variance of the MOE were also statistically shown to develop appropriate machine strength grading procedures [2]. A three-dimensional finite element model was suggested to investigate the impact of knots on the strength decrease of Norway spruce wood. The knot's cross-section is considered oval, and its axis might be nonlinear. The diving angle can be used to illustrate the radial fibre deviation's orientation [3]. When assessing the strength and failure mechanism of wood specimens, the diving angle, also known as an out-of-plane angle, must be considered; it can approach the description of fibre orientation out of the plane of the beam face [44]. Furthermore, considering the existence of knots and their related fibre deviations, a three-dimensional finite element model was utilized to estimate the mechanical properties of Norway Spruce wood boards [45].

Analytical methods can also be used to determine the knot geometry and related fibre deviation. A mathematical model was proposed to characterize the knots and their accompanying fibre deviation boundaries in three dimensions, assuming that second and third-order polynomial functions might approximate the borders. The tangent $R(P, R_{io})$ is used to calculate the fibre deviations; this can be approximated by the distance between the tree's pith and a specific growth layer near the knot (R_{io}), the distance between the knot's centre and any examined location (P), and other variables related to the type of wood member [42].

The most significant stress concentration is usually seen near the member's edge, where knots form. The knots in the centre of the member have the lowest stress concentrations. The area behind the knot is also thought to be inefficient and incapable of overcoming tension [46]. The impact of knot size and position on the behaviour of structural wood components was investigated using a two-dimensional parametric finite element model. Openings and cylinders were used to estimate the knots.

On the other hand, these models do not account for the effect of dive angles [47]. Furthermore, the impact of the

knot's size, placement, and diving angle on bending was parametrically investigated using elliptical oblique and rotating cones [48]. Knot density and size effect on bending strength and flexural stiffness was also studied [49].

Knots in structural wood are considered a severe problem. When identified in the tension zone, they decrease the stiffness and ultimate capacity of wood components. In particular numerical research, knots were represented as holes. Due to the existence of knots represented by holes at the tension zones of the beams during bending, [50] examined the local stress concentration quantitatively. They discussed how the size and location of the hole affected the stress distribution in Pinewood, which was treated as a linear elastic orthotropic material. The distance between the knot's centre and the base surface, its diameter, and the quantity of loads were connected to the distribution of normal stresses. The stress ratio between the weakened and non-weakened beams decreases as getting closer to the neutral axis. Another study discovered a reduction in bending stiffness when knots were also represented by apertures, with a 50 mm diameter providing an 83% reduction in bending stiffness [1].

Furthermore, theoretical and experimental research investigations have shown that openings can simulate knots. The authors found no significant differences in the timber beams' estimated ultimate forces and strengths (MOR, MOE, maximum force, and deflection). On the other hand, an opening would not offer a signal of impending failure. Natural knots of different locations, sizes, and forms were found in the beams, and each sample was then defected by an opening with a matching fibre pattern. When both techniques' load-deflection curves were evaluated, they displayed comparable properties. The final loads were not appreciably different [51].

A comparable investigation was also conducted. To investigate the behaviour of recycled timbers with fastener holes and their effects on ultimate flexural capacities, the authors developed an analytical two-dimensional finite element model combined with the Tsai-Wu strength theory for anisotropic materials, which was validated with a destructive four-point bending experimental investigation. The distance between the edge of the hole and the extreme compression or tension fibres should not be less than 6 mm. On the ultimate flexural capacity of the member, the effects of different bolt hole sizes positioned at the midspan of the beam with variable locations relative to the edge of the compression and tension edges were investigated. The fastener hole at the beam's mid-span provides the section's most significant flexural resistance decrease. For failure prediction, a "load-stepping" technique was used, in which every failed element (reaching one according to Tsai-Wu) was removed from the analysis and treated as a localized failure, resulting in a "net effective section" that was then used in the subsequent analysis step. The load-deflection curves were recorded using the load-step method until the global failure was attained. 25.4 mm holes with centres 19 mm (6.3 mm away from the edge) and 12.7 mm (touch the

edge) away from the tension edge had the lowest ultimate load capacity. Because these holes are so near to the tension edge, it may be concluded that a hole so close to the edge has similar consequences as one that contacts the edge [52].

On the other hand, Knots are depicted as a cone or cylinder with a diving angle perpendicular to the longitudinal wood fibre. Because the inner geometry of the knot is unknown, in most cases, assumptions and approximations should be used, such that a cone can be used to depict the knot with an inclination toward the log's pith. Examples of such approximations are shown in [53]. Using finite element modelling and an orthotropic elastic-plastic constitutive equation for wood in the plane stress state, the final flexural capacity of defective *Pinus sylvestris* L. beams exposed to four-point bending was projected. The location and magnitude of knots and grain variations were used to predict the rupture region. Experiments were also conducted to validate the models [54]. A knot represented by an opening, an adherent knot attached to the rest of the beam, and a partial contact knot with the rest of the beam were all modelled. The first model was the most accurate in predicting the bending failure load for the knots in the tension zone. A related study developed a three-dimensional analytical material model to anticipate the behaviour of timber beams while accounting for the effects of any existing knots in the form of elliptical, rotating, or oblique cones [43]. Because the material qualities of timber, such as strength and stiffness, are susceptible to local fibre orientations, the impact of grain deviation caused by the presence of the knot must be investigated. Knots frequently cause a stress disturbance in their immediate surroundings, and the resulting grain deviations reduce tensile strength and cause stress redistribution. Nonetheless, they have a negligible impact on compression strength parallel to the undisturbed grain direction.

The main objective of this work is to investigate the effect of two closely spaced conical knots and related fibre deviations on the ultimate flexural capacity of Norway spruce wood beams subjected to four-point bending using parametric finite element analysis. The study seeks to determine the effects of a knot adjusted in a vicinity of a fixed knot located at the mid-span in both directions, X and Y.

Methodology

The ultimate objective is to determine the influence of two closely-spaced knots on the failure modes of timber beams. For a correct evaluation, the elastic stiffness and modulus of elasticity parallel to grains were determined from a linear regression line determined from the load-deflection curves to validate the numerical models.

After that, the specimens were tested for bending. Two pilots undefected (without knots) and four defected (with knots) beams were tested to determine their load-bearing capacities. In addition to the quasi-static bending tests, compressive tests were conducted to verify the fundamental characteristics of wood. The rest of the material properties were adopted from literature.

The knot size and position were measured based on visual inspection. Data were implemented into the three-dimensional F.E. model for validation, considering the knots and related fibre deviations.

Experimental

The experimental program considered four-point quasi-static bending testing on rectangular wood beams. Two beams were tested, one with knots and the other without. Compressive tests were undertaken in addition to the quasi-static bending tests to validate the main characteristics of wood in compression.

The Norway spruce beams had a length of 1000 mm and a rectangular cross-section of 100 mm × 100 mm. At the time of testing, the moisture content was 12 per cent. Visual inspection of the knot-free specimens revealed faults, primarily in the form of knots, which were confirmed to be on the compression side if available. No severe flaws or defects were found, such as drying splits and biological degradation. The knotted specimens contain knots of different sizes and positions in the tension zone.

The physical measurements and weights of each component were measured and documented. The average material properties for the timber material are shown in **Table 1**.

Table 1. Average material properties for Nordic Spruce timber [8-11].

Material property name	Value
Moisture content	12%
Modulus of elasticity (E_L)	10900 MPa
Modulus of elasticity (E_T)	420 MPa
Modulus of elasticity (E_R)	640 MPa
Shear modulus (G_{LR})	580 MPa
Shear modulus (G_{LT})	590 MPa
Shear modulus (G_{RT})	26 MPa
Poisson's ratio (ν_{LR})	0.39
Poisson's ratio (ν_{LT})	0.49
Poisson's ratio (ν_{RT})	0.64
Longitudinal compression strength (σ_{c0})	40.6 MPa
Tangential compression strength (σ_{c90})	4.7 MPa
Tensile strength parallel to grain (σ_{TL})	99.1 MPa
Tensile strength perpendicular to grain (σ_{TR})	4.9 MPa
Tensile strength perpendicular to grain (σ_{LR})	2.8 MPa
Shear strength (τ_{LR})	6.1 MPa
Shear strength (τ_{LT})	4.4 MPa
Shear strength (τ_{RT})	1.6 MPa
Modulus of rupture	67.7 MPa

The ASTM D143 standard was used to conduct the bending tests, which consisted of a series of quasi-static four-point bending examinations. The load was delivered at a rate of 7 mm/min via a crosshead displacement control performed with a standard MTS testing equipment with 600 kN. As demonstrated in **Fig. 2**, a single actuator in the beam's centre transmitted the load to the two points of the beam. The specimens were placed on supports with a 900 mm clear span. See **Table 2** for specimen specifications and test results.



Fig. 2. Four-point bending test.

Table 2. Test specimens - bending. Ultimate loads (KN) and deflections (mm).

Specimen	Characteristics	Displacement (mm)	Load (KN)
S1	Knot-free	34.03	67.24
S2	Knot-free	35.65	67.24
S3	knotted	21.70	51.06
S4	knotted	18.22	42.82
S5	knotted	20.80	50.68
S6	knotted	23.88	43.23

This investigation also included parallel-to-grain compressive testing to assess the wood's inelastic compression characteristics. The tests were carried out using an ATS mechanics testing machine with crosshead displacement control at a 0.6 mm/min rate. Ten different specimens were evaluated, whose dimensions (height × width × length) of 30 mm × 30 mm × 180 mm. The axial contractions were recorded, and the compression stress-strain diagram was obtained, which will be used to define the parameter needed for the bi-linear compression stress-strain diagram. The curves representing the axial contractions are illustrated in Fig. 3.

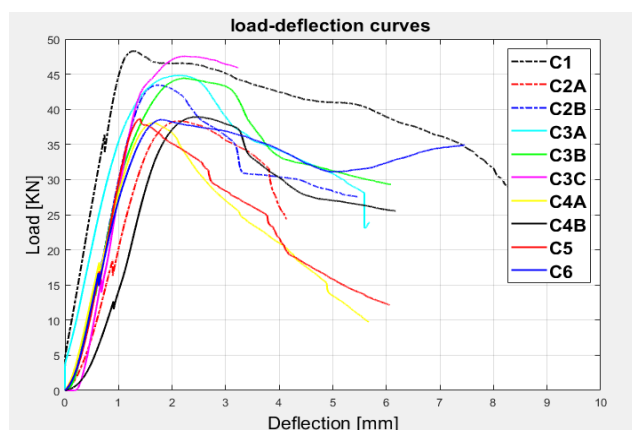


Fig. 3. Axial contraction for all specimens (compression test).

FEM analysis of 4-point bending tests

The results from the tests were used to calibrate finite element models so that the influence of the knots on the flexural behaviour of the wood beams could be quantitatively evaluated. Furthermore, to accurately create three-dimensional numerical representations for the knots and related fibre deviations.

The following finite element models were evaluated: (i) 3D models of beams without knots; (ii) 3D models of knotted beams with one knot located in the tension side at a distance of 5 mm far from the extreme tension fibres to the bottom of the knots, (iii) parametric 3D models of knotted beams with two-closely spaced knots with a centre to centre distance d (in the longitudinal direction) and v (in the vertical direction). No finite contact elements were used for the boundary conditions at the supports and the centre loading. Furthermore, as illustrated in Fig. 4, the boundary conditions were applied directly to the nodes located at 50 mm, and 950 mm from both beams' ends. The three-dimensional computational models were built using the ANSYS APDL language supplied by the general-purpose FEA program ANSYS.

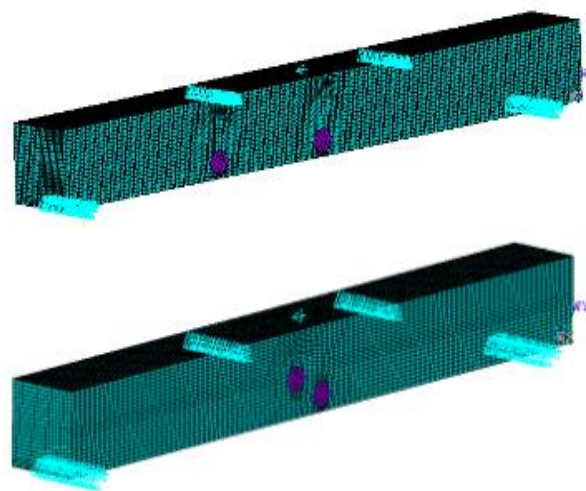


Fig. 4. FEM model. Loading and boundary conditions.

Constitutive modelling

Using the general form of Hooke's law, an elastic orthotropic constitutive relationship for wood material was established in the linear range:

$$\sigma = D\varepsilon,$$

where σ is the stress vector in each of the three orthotropic directions, ε is the associated strain vector, and D is the orthotropic stiffness matrix made up of nine different material qualities of the wood species. The rest of the attributes were taken from the literature. Furthermore, both compression and tension were considered to have the same modulus of elasticity.

Wood beams show a linear elastic-quasi rigid response when subjected to tensile loads. Wood shows both linear-elastic and nonlinear inelastic behaviour when compressed. Consequently, the nonlinear behaviour of the wood beams was replicated using the generalized anisotropic Hill potential model. The model has varied yield strengths in tension and compression, and it might react differently in the x , y , and z dimensions.

A bilinear anisotropic stress-strain relationship allows the different components of tension and compression to yield stresses. Uniaxial tensile and compressive stress-strain curves characterize the material behaviour in three orthogonal directions and shear stress-engineering shear strain curves in the corresponding directions. A bilinear response is studied for each direction. The starting slope of the curve is used to compute the material's elastic moduli. At the desired yield stress, the curve continues down the second slope indicated by the tangent modulus. The experiment may be used to determine the compression yield stress and tangent modulus in the grain direction.

The knot-related fibre pattern differs significantly from that of clear wood. The three orthogonal directions (Longitudinal L , Radial R , Tangential T) that are characteristic in transparent timber describe the orthotropic behaviour of wood. On the other hand, Knots have no such fibre pattern since the fibres are aligned in unpredictable orientations, resulting in a disordered arrangement. It means that the material has comparable qualities in all directions; hence isotropy is the best way to describe its behaviour.

Material properties are unaffected by loading rates. The effects of the environment on the beams' structural behaviour, such as moisture and temperature, were not considered. **Table 1** summarizes the material attributes used in the numerical models.

Constitutive modelling

The wood species were represented using three-dimensional solid elements (SOLID 45). The eight-node element contains three translational degrees of freedom per node, which corresponds to the orthotropic properties of timber beams. The beam was divided into 113,250 finite elements. Boundary conditions were applied directly to the nodes to depict the simply-supported condition. The same element type was used to simulate the behaviour of the knots. No contact elements were specified between the clear wood and the knots.

The tested specimens in bending were divided up into multiple plies of 10 mm each in the direction parallel to the grains until they reached the tip of the knot to establish the natural three-dimensional fibre paradigm in its vicinity. To reproduce the precise knot shape and related fibre deviations, measurements of the grains for each ply were obtained and reproduced in ANSYS to establish the three-dimensional finite element models. All of the knots studied were conical in form (see **Fig. 5**).

As wood is a highly anisotropic material, the orientation of the fibres has a significant impact on the mechanical properties. Because the fibre pattern surrounding a knot deviates so far from the regular parallel direction of pure wood, it becomes essential in terms of stress conditions, capacity, and other factors. The orthotropic material's longitudinal orientation (L) should be aligned with the fibres in the model from a technical standpoint. It is worth noting that the solid element in the ANSYS program has a default orientation that is parallel to the global Cartesian coordinate system. Therefore, the material coordinate system must be independently orientated for each finite element.

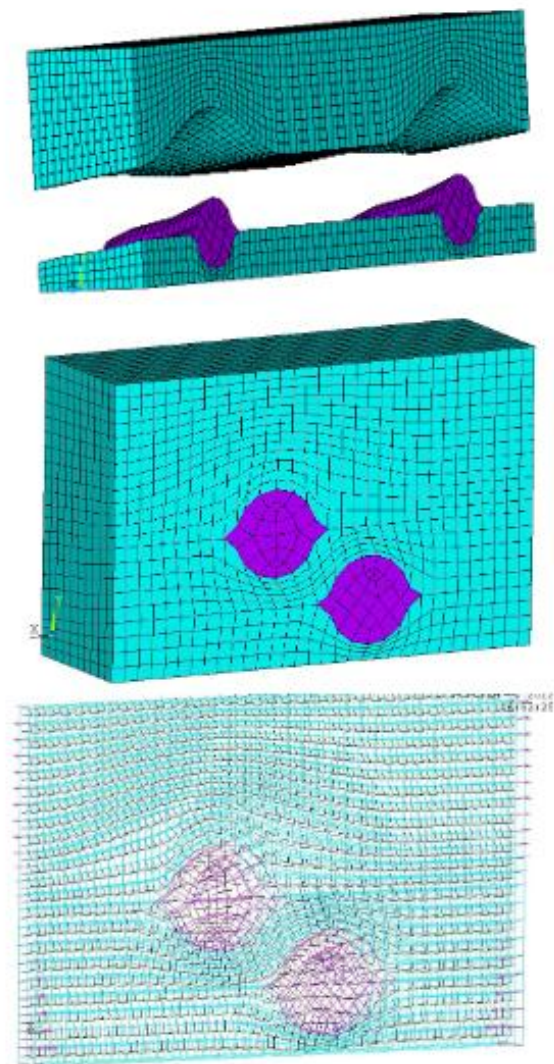


Fig. 5. Three-dimensional representation of knots and related fibre deviations. (a) $v = 0$, (b) $v = 25$ mm, (c) fibre orientations.

Failure criterion

Tension is a typical reason for wood element failure because it causes the plastic capacity of the beam compression zone to be underused. As a result of weight,

micro-cracks develop into macro-cracks, causing irreversible damage to the timber beams. The Tsai-Wu strength hypothesis is the most widely recognized failure criteria for determining anisotropic materials' ultimate load-bearing capability.

ANSYS uses the inverse of the strength ratio as the TWSR failure criteria for consistency. If the TWSR criteria value is greater than 1, it indicates failure. The TWSR indices, on the other hand, are best regarded as damage initiation indices since they provide information on the beginning of failure in the specimen under consideration. It is necessary to determine the maximum permissible material strength values (stresses or strains).

Results and discussion

Load-deflection response and failure assessment

The experimental load-deflection curves for each tested specimen were used to calibrate the rate-independent inelastic material model. The specimens *S1* and *S2* for knot-free beams were selected and evaluated to serve as references.

In tension, all knot-free specimens failed due to the longitudinal splitting of fibres parallel to the grains. Before the global collapse, intangible local damages began. Knots, if any, were ensured to be located in the compression zone of the beams, demonstrating that knots and related fibre deviations have a negligible impact on the compression strength of wood beams.

The experiments revealed that tensile failure was confined to the knot, followed by a complete progressive failure with a significant reduction in the ultimate capacity, demonstrating the importance of local fibre waviness caused by knots in wood beams. The load-deflection curve has a minor non-linearity due to early tension failure caused by local fibre deviation around the knot. Furthermore, local premature tensile failure followed by a global beam failure prevents the full use of timber's compression capacity; hence, the ductility is not fully utilized.

After tension fibres have ruptured, horizontal cracks typically occur towards the midway. It suggests that a weak area in the wood substance is most likely to blame for the failure. The failure usually starts in the tension zone and progresses to the weaker part of the beam. The loss of ductility further underscores the difference between knot-free and knotted beams. It lowers the tensile strength of the timber cross-section, eventually causing it to collapse.

The parametric study

The effect of a single knot is first studied parametrically positioned at the longitudinal axis (*x-axis*) for evaluating the failure initiation at the adjacent knot concerning the centre-to-centre distance *d*. All the beams were subjected to four-point bending with a displacement-controlled loading of 25 mm. The material properties adopted are shown in **Table 1**.

Effect of a single knot

The effect of a single knot (*knot-1*) located at the mid-span of the beam in the tension zone whose diameter $D = 30$ mm, length $L = 50$ mm, diving angles equal to zero, and 5 mm the distance from the extreme tension fibre to the knot bottom. **Fig. 6**. The study was performed to serve as a reference when evaluating the effects of another knot located at a different location within the beam.

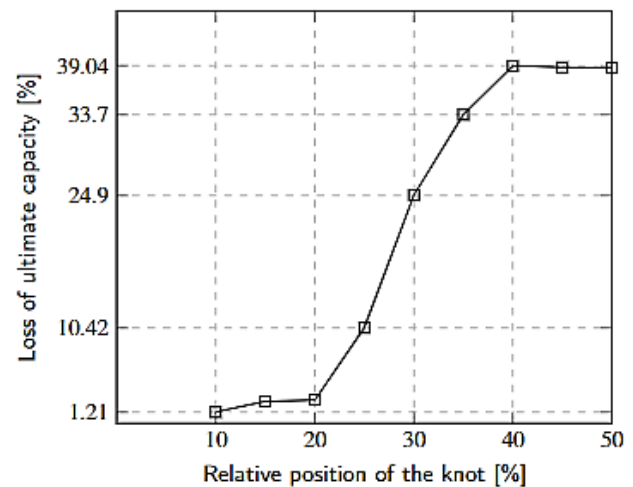


Fig. 6. Loss of capacity relative to knot position along *x-axis*.

According to the findings, when a knot is detected near supports, the consequences on flexural behaviour are negligible. When the knot was placed at a distance of 25% of the beam's complete length, there was a noticeable drop in ultimate capacity of 10.42%. The loss of load-bearing capacity reached a maximum of 39% when the knot was in the middle of the beam. Failures are reproduced in the disturbed fibre zone around the knot. However, a typical bending failure occurs when the knot is close to the support.

Effect of two knots

The lack of ductility underlines a substantial differential between knotted and non-knotted wood beams. The presence of the knot causes early tensile failure in the wood at the same stress level. As a result, the maximum load is carried out at a lower level. One of the knots is fixed to the mid-span of the beam, where we expect the highest loss of load-bearing capacity, and the other knot is moving according to two different scenarios:

- I. Two closely spaced knots with varying centre-to-centre distance *d* only in the longitudinal direction (*x-axis*), see **Fig. 7(a)**. The distance from the edge of the knots to the extreme tension fibre is $b = 5$ mm.
- II. Two closely spaced knots with varying centre-to-centre distance in the longitudinal (*d*) and vertical ($v = 25$ mm) directions (*x and y-axis*), see **Fig. 7(b)**.

Both knots have a conical shape with a length of $L = 50$ mm, a visible diameter of $D = 30$ mm, and vertical and

horizontal diving angles of zero degrees. All beams in the parametric study are subjected to four-point bending under displacement-controlled loading of 20 mm.

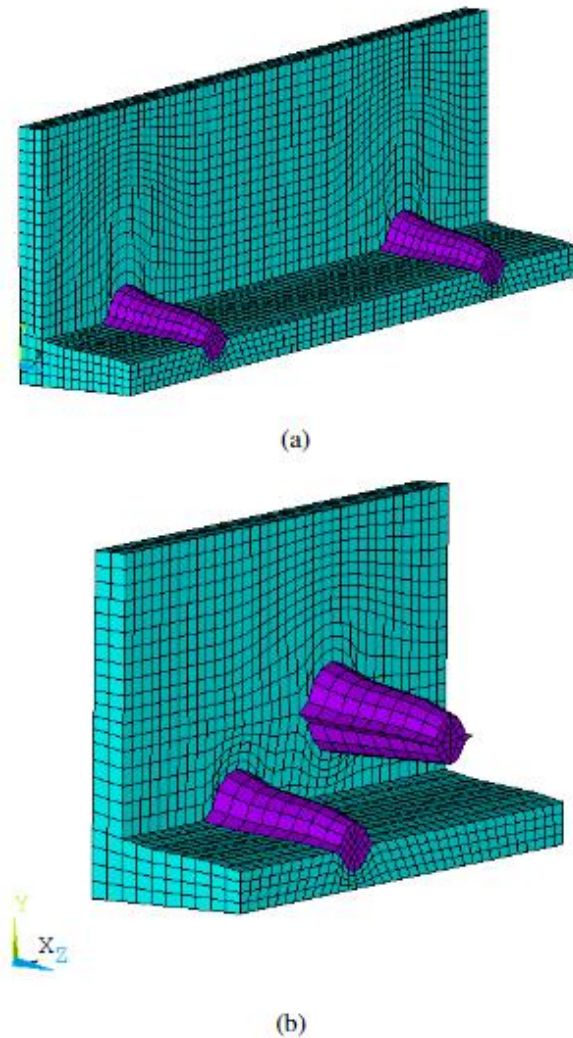


Fig. 7. Two closely-spaced knots with horizontal and vertical center to center distances d and v . (a) $d = 400$ mm and $v = 0$, (b) $d = 50$ mm and $v = 25$ mm.

In the first case, where v is zero, the failure initiation at *knot-1* is not affected by the presence of an adjacent knot. The Tsai Wu predicted failure at the same load level for both knots. Results show that the percentage of loss of bearing capacity is similar to a single knot located at those two different positions, see **Fig. 6**.

For the second case, the presence of an adjacent knot caused a failure initiation at the adjacent knot at a higher load level. The area between knots was subjected to high shear deformation. The shear failure mechanism started before reaching the ultimate tensile capacity of the beam, see **Fig. 8**. The clear wood part between the knots is considered ineffective. The shear failure is dominant if the centre-to-centre distance $d < 3 \times D$. Beyond this value, tension will cover the failure only.

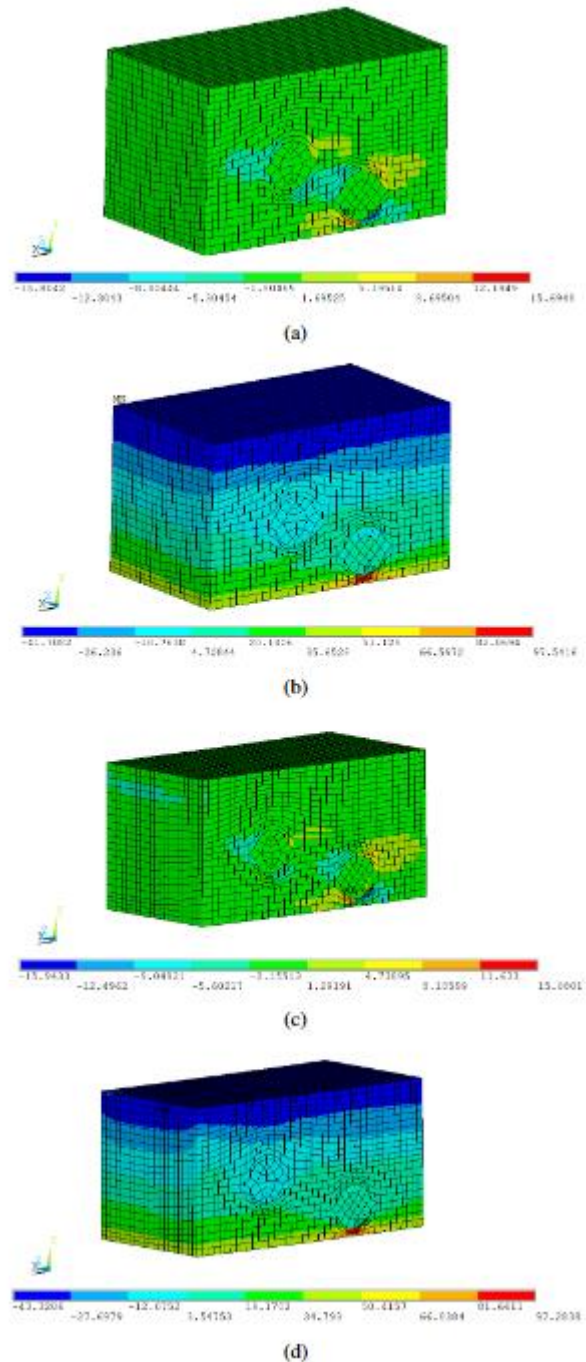


Fig. 8. Normal and shear stress distribution at the same load level that causes the ultimate tensile strength. (a) shear stress - (b) Normal stress for for $d = 1.5 \times D$; (c) shear stress - (d) Normal stress for for $d = 2.5 \times D$.

Conclusion

The knot shape and accompanying fibre variations were predicted adequately in this study utilizing numerical simulations. To validate the models, four-point bending tests were performed on Spruce timber. The numerical models correctly followed the three-dimensional local grain variations induced by the knot's presence without approximations, resulting in a perfect match between the

simulated and observed load-deflection curves. Because of the early tension and shear failures caused by the presence of knots in the timber beam, the compression capacity is ineffectively utilized. The following is a summary of the findings:

- (i) To better understand the effect on the flexural behaviour of timber beams, the 3D knot and related fibre variations were parametrically modelled.
- (ii) Visual inspections can be used to validate the model. The user needs to enter the size and location of the knots for the 3D numerical model.
- (iii) For the case where the vertical centre-to-centre distance between the two knots is $v = 0$, the load level that initiates the failure does not depend on the presence of an adjacent knot.
- (iv) For $v = 25$ mm. If the centre-to-centre distance $d = 3 \times D$, the clear wood section between the knots is deemed ineffectual, and shear failure is considered dominating. Beyond this level, only tension will conceal the failure.

Acknowledgements

The presented work was conducted with the financial support of the K138615 project of the Hungarian National Research, Development, and Innovation Office.

Conflicts of interest

The authors declare that they have no known competing financial interests or personal relationships that could have appeared to influence the work reported in this paper.

Keywords

Timber, knot, FEM, fibre deviation

Supporting information

Supporting information is available online at the journal website.

References

1. Burawska, I.; Mohammadi, A.H.; Widmann, R.; Motavalli, M.; Local reinforcement of timber beams using D-shape CFRP strip. *SMAR* (2015). [https://www.dora.lib4ri.ch/empa/islandora/object/empa%3A9494/datastream/PDF/Burawska-2015-Local reinforcement of timber beams-\(published version\).pdf](https://www.dora.lib4ri.ch/empa/islandora/object/empa%3A9494/datastream/PDF/Burawska-2015-Local%20reinforcement%20of%20timber%20beams-(published%20version).pdf)
2. Hu, M.; Studies of the fibre direction and local bending stiffness of norway spruce timber: for application on machine strength grading. PhD thesis, Linnaeus University Press (2018). <https://doi.org/10.3390/icem18-05426>
3. Foley, C.; A three-dimensional paradigm of fiber orientation in timber. *Wood science and technology*, **2001**, *35*(5), 453-465. <https://doi.org/10.1007/s002260100112>
4. Borri, A.; Corradi, M.; Vignoli, A.; New materials for strengthening and seismic upgrading interventions. In: *International Workshop Ariadne*, **2002**, vol. 10, pp. 22-28. http://www.itam.cas.cz/ARCCHIP/w10/w10_borri.pdf
5. Liu, J.; Evaluation of the tensor polynomial strength theory for wood. *Journal of Composite Materials*, **1984**, *18*(3), 216-226. <https://doi.org/10.1177/002199838401800302>
6. Hasebe, K.; Usuki, S.; Application of orthotropic failure criterion to wood. *Journal of Engineering Mechanics*, **1989**, *115*(4), 867-872. [https://doi.org/10.1061/\(asce\)0733-9399\(1989\)115:4\(867\)](https://doi.org/10.1061/(asce)0733-9399(1989)115:4(867))
7. Patton-Mallory, M.; Pellicane, P.J.; Smith, F.W.; Modeling bolted connections in wood. *Journal of Structural Engineering*, **1997**, *123*(8), 1054-1062. [https://doi.org/10.1061/\(ASCE\)0733-9445\(1997\)123:8\(1054\)](https://doi.org/10.1061/(ASCE)0733-9445(1997)123:8(1054))
8. Green, D.W.; Winandy, J.E.; Kretschmann, D.E.; Mechanical properties of wood. wood handbook : wood as an engineering material. Technical Report General technical report FPL; GTR-113, USDA Forest Service, Forest Products Laboratory, Madison, WI, USA (1999). <https://www.fpl.fs.fed.us/documnts/fplgtr/fplgtr113/ch04.pdf>
9. Rijdsdijk, J.F.; Laming, P.B.; Physical and Related Properties of 145 Timbers: Information for Practice. Springer, (1994). <https://books.google.hu/books?id=CFVDSWPUMIsC>
10. Okstad, T.; K arstad, H.; The mechanical properties of spruce wood (picea abies l. karst.) in northern norway. Meddelelser fra Norsk Institutt for Skogforskning (Norway) (1985).
11. Kristian, B.D.; Mechanical properties of clear wood from norway spruce. PhD thesis, Norwegian University of Science and Technology (2009). <http://hdl.handle.net/11250/236422>
12. Tingley, D.A.; The stress-strain relationships in wood and fiber-reinforced plastic laminae of reinforced glued-laminated wood beams. PhD thesis, Oregon State University (1997).
13. Kirilin, C.P.; Experimental and finite-element analysis of stress distributions near the end of reinforcement in partially reinforced glulam. Master's thesis, Oregon State University, USA. (1996). <http://hdl.handle.net/1957/12262>
14. Serrano, E.; Glued-in rods for timber structures - A 3D model and finite element parameter studies. *International Journal of Adhesion and Adhesives*, **2001**, *21*(2), 115-127. [https://doi.org/10.1016/S0143-7496\(00\)00043-9](https://doi.org/10.1016/S0143-7496(00)00043-9)
15. Kasal, B.; Heiduschke, A.; Radial reinforcement of curved glue laminated wood beams with composite materials. *Forest Products Journal*, **2004**, *54*(1), 74-79.
16. Khelifa, M.; Vila Loperena, N.; Bleron, L.; Khennane, A.; Analysis of CFRP-strengthened timber beams. *Journal of Adhesion Science and Technology*, **2014**, *28*(1), 1-14. <https://doi.org/10.1080/01694243.2013.815096>
17. Nowak, T.P.; Jasienko, J.; Czepizak, D.; Experimental tests and numerical analysis of historic bent timber elements reinforced with CFRP strips. *Construction and Building Materials*, **2013**, *40*, 197-206. <https://doi.org/10.1016/j.conbuildmat.2012.09.106>
18. Nadir, Y.; Nagarajan, P.; Ameen, M., et al.; Flexural stiffness and strength enhancement of horizontally glued laminated wood beams with GFRP and CFRP composite sheets. *Construction and Building Materials*, **2016**, *112*, 547-555. <https://doi.org/10.1016/j.conbuildmat.2016.02.133>
19. Fiorelli, J.; Dias, A.A.; Glulam beams reinforced with FRP externally-bonded: Theoretical and experimental evaluation. *Materials and Structures*, **2011**, *44*(8), 1431-1440. <https://doi.org/10.1617/s11527-011-9708-y>
20. Johnsson, H.; Blanksv ard, T.; Carolin, A.; Glulam members strengthened by carbon fibre reinforcement. *Materials and Structures*, **2007**, *40*(1), 47-56. <https://doi.org/10.1617/s11527-006-9119-7>
21. Schober, K.U.; Harte, A.M.; Klinger, R.; Jockwer, R.; Xu, Q.; Chen, J.-F.; FRP reinforcement of timber structures. *Construction and Building Materials*, **2015**, *97*, 106-118. <https://doi.org/10.1016/j.conbuildmat.2015.06.020>
22. Li, Y.F.; Tsai, M.J.; Wei, T.F.; Wang, W.C.; A study on wood beams strengthened by FRP composite materials. *Construction and Building Materials*, **2014**, *62*, 118-125. <https://doi.org/10.1016/j.conbuildmat.2014.03.036>
23. Moses, D.M.; Prion, H.G.; Anisotropic plasticity and failure prediction in wood composites. Ansys. net (online) (2002)
24. Madenci, E.; Guven, I.; The Finite Element Method and Applications in Engineering Using ANSYS®. Springer, (2015). <https://books.google.hu/books?id=aJKebgAAQBAAJ>
25. Hill, R.; A theory of the yielding and plastic flow of anisotropic metals. Proceedings of the Royal Society of London. Series A. Mathematical and Physical Sciences, **1948**, *193*(1033), 281-297. <https://doi.org/10.1098/rspa.1948.0045>
26. Shih, C.; Lee, D.; Further developments in anisotropic plasticity. *Journal of Engineering Materials and Technology*, **1978**, *100*(3), 294-302. <https://doi.org/10.1115/1.3443493>

27. Valliappan, S.; Boonlaulohr, P.; Lee, I.; Nonlinear analysis for anisotropic materials. *International Journal for Numerical Methods in Engineering*, 1976, 10(3), 597-606. <https://doi.org/10.1002/nme.1620100309>
28. Buchanan, A.H.; Bending strength of lumber. *Journal of Structural Engineering*, 1990, 116(5), 1213-1229. [https://doi.org/10.1061/\(asce\)0733-9445\(1990\)116:5\(1213\)](https://doi.org/10.1061/(asce)0733-9445(1990)116:5(1213))
29. Cizmar, D.; Sørensen, J.D.; Kirkegaard, P.H.; Rajčič, V.; Robustness analysis of a timber structure with ductile behaviour in compression. In: Proceedings of the Final Conference of COST Action TU0601: Robustness of Structures, pp. 17-32, 2011. Czech Technical University, Prague. <https://vbn.aau.dk/en/publications/robustness-analysis-of-a-timber-structure-with-ductile-behaviour>
30. Raftery, G.M.; Harte, A.M.; Nonlinear numerical modelling of FRP reinforced glued laminated timber. *Composites Part B: Engineering*, 2013, 52, 40-50. <https://doi.org/10.1016/j.compositesb.2013.03.038>
31. Mascia, N.T.; Lahr, F.A.R.; Remarks on orthotropic elastic models applied to wood. *Materials Research*, 2006, 9(3), 301-310. <https://doi.org/10.1590/S1516-14392006000300010>
32. Hermanson, J.C.; The Triaxial Behavior of Redwood Using a New Confined Compression Device. PhD Thesis, The University of Wisconsin, Madison, USA., 1996. <https://books.google.hu/books?id=LKSFAAAAMAAJ>
33. Milch, J.; Tippner, J.; Sebera, V.; Brabec, M.; Determination of the Elastoplastic Material Characteristics of Norway Spruce and European Beech Wood by Experimental and Numerical Analyses. *Holzforschung*, 2016, 70(11), 1081-1092. <https://doi.org/10.1515/hf-2015-0267>
34. Kretschmann, D.E.; Mechanical properties of wood. wood handbook : Wood as an engineering material. Technical Report General Technical Report FPL; GTR-190, USDA Forest Service, Forest Products Laboratory, Madison, WI, USA (2010). https://www.fpl.fs.fed.us/documnts/fplgtr/fplgtr190/chapter_05.pdf
35. Mitsuhashi, K.; Poussa, M.; Puttonen, J.; Method for predicting tension capacity of sawn timber considering slope of grain around knots. *Journal of Wood Science*, 2008, 54(3), 189-195. <https://doi.org/10.1007/s10086-007-0941-5>
36. Mihashi, H.; Navi, P.; Sunderland, H.; Itagaki, N.; Ninomiya, S.; Micromechanics of knot's influence on tensile strength of Japanese cedar. In: 1st Rilem Symposium on Timber Engineering, Volume Stockholm, Sweden, pp. 181-190 (1999). ISBN: 2912143101, 9782912143105
37. Briggert, A.; Hu, M.; Olsson, A.; Oscarsson, J.; Tracheid effect scanning and evaluation of in-plane and out-of-plane fiber direction in Norway spruce timber. *Wood and Fiber Science*, 2018, 50(4), 411-429. <https://doi.org/10.22382/wfs-2018-053>
38. Cramer, S.; Shi, Y.; McDonald, K.; Fracture modeling of lumber containing multiple knots. In: Proceedings of the International Wood Engineering Conference 1996, October 28-31, New Orleans, La, pp. 288-294 (1996). <https://www.fpl.fs.fed.us/documnts/pdf1996/crame96b.pdf>
39. Ekevad, M.; Method to compute fiber directions in wood from computed tomography images. *Journal of Wood Science*, 2004, 50(1), 41-46. <https://doi.org/10.1007/s10086-003-0524-z>
40. Journal, E.I.; A new tree biology - facts, photos and philosophies and their problems and proper care. alex l. shigo, xiv + 595 pp., illus., 1986 (hard cover). *IAWA Journal*, 1988, 9(3), 292-292. <https://doi.org/10.1163/22941932-90001082>
41. Wangaard, F.F.; The mechanical properties of wood, 1950.
42. Foley, C.; Modeling the effects of knots in structural timber. PhD thesis, Lund University (2003).
43. Guindos, P.; Guaita, M.; A three-dimensional wood material model to simulate the behavior of wood with any type of knot at the macro-scale. *Wood Science and Technology*, 2013, 47(3), 585-599. <https://doi.org/10.1007/s00226-012-0517-4>
44. Stahl, D.C.; Cramer, S.M.; McDonald, K.; Modeling the effect of out-of-plane fiber orientation in lumber specimens. *Wood and Fiber Science*, 2007, 22(2), 173-192.
45. Lukacevic, M.; Kandler, G.; Hu, M.; Olsson, A.; Fußl, J.; A 3D model for knots and related fiber deviations in sawn timber for prediction of mechanical properties of boards. *Materials & Design*, 2019, 166, 107617. <https://doi.org/10.1016/j.matdes.2019.107617>
46. Cramer, S.; Goodman, J.; Model for stress analysis and strength prediction of lumber. *Wood and Fiber Science*, 1983, 15(4), 338-349.
47. Banó, V.; Arriaga, F.; Guaita, M.; Determination of the influence of size and position of knots on load capacity and stress distribution in timber beams of pinus sylvestris using finite element model. *Biosystems Engineering*, 2013, 114(3), 214-222. <https://doi.org/10.1016/j.biosystemseng.2012.12.010>
48. Guindos, P.; Guaita, M.; The analytical influence of all types of knots on bending. *Wood Science and Technology*, 2014, 48(3), 533-552. <https://doi.org/10.1007/s00226-014-0621-8>
49. Grant, D.; Anton, A.; Lind, P.; Bending strength, stiffness, and stress-grade of structural pinus radiata: effect of knots and timber density. *New Zealand Journal of Forestry Science*, 1984, 14(3), 331-348.
50. Burawska, I.; Tomusiak, A.; Turski, M.; Beer, P.; Local concentration of stresses as a result of the notch in different positions to the bottom surface of bending solid timber beam based on numerical analysis in solidworks simulation environment. *Annals of Warsaw University of Life Sciences- SGGW, Forestry and Wood Technology*, 2011, 73, 192-198.
51. Burawska, I.; Zbiec, M.; Kalicki, J.; Beer, P.; Technical simulation of knots in structural wood. *Annals of Warsaw University of Life Sciences- SGGW, Forestry and Wood Technology*, 2013, 82.
52. Williams, J.M.; Fridley, K.J.; Cofer, W.F.; Falk, R.H.; Failure modeling of sawn lumber with a fastener hole. *Finite Elements in Analysis and Design*, 2000, 36(1), 83-98. [https://doi.org/10.1016/S0168-874X\(00\)00010-X](https://doi.org/10.1016/S0168-874X(00)00010-X)
53. Kandler, G.; Lukacevic, M.; Fußl, J.; An algorithm for the geometric reconstruction of knots within timber boards based on fibre angle measurements. *Construction and Building Materials*, 2016, 124, 945-960. <https://doi.org/10.1016/j.conbuildmat.2016.08.001>
54. Banó, V.; Arriaga, F.; Soil'an, A.; Guaita, M.; Prediction of bending load capacity of timber beams using a finite element method simulation of knots and grain deviation. *Biosystems Engineering*, 2011, 109(4), 241-249. <https://doi.org/10.1016/j.biosystemseng.2011.05.008>

Authors biography



Prof András Lengyel is an associate professor at the Department of Structural Mechanics, Budapest University of Technology and Economics. He has PhD degree in Engineering at the University of Oxford. He has co-authored 39 journal and conference papers.



Khaled Saad has a MSc degree in Civil Engineering at Budapest University of Technology and Economics. He is a PhD student at the Department of Structural Mechanics under the supervision of András Lengyel working on strengthening timber beams with fibre reinforced polymers.